

## Study of the Time Response of a Simulated Hydroelectric System

This content has been downloaded from IOPscience. Please scroll down to see the full text.

2014 J. Phys.: Conf. Ser. 570 052003

(<http://iopscience.iop.org/1742-6596/570/5/052003>)

View [the table of contents for this issue](#), or go to the [journal homepage](#) for more

Download details:

IP Address: 151.42.29.120

This content was downloaded on 18/12/2014 at 15:09

Please note that [terms and conditions apply](#).

# Study of the Time Response of a Simulated Hydroelectric System

**S. Simani, S. Alvisi, M. Venturini**

Dipartimento di Ingegneria, Università degli Studi di Ferrara. Via Saragat 1E – 44122 Ferrara (FE), Italy

E-mail: {[silvio.simani](mailto:silvio.simani@unife.it),[stefano.alvisi](mailto:stefano.alvisi@unife.it),[mauro.venturini](mailto:mauro.venturini@unife.it)}@unife.it

**Abstract.** This paper addresses the design of an advanced control strategy for a typical hydroelectric dynamic process, performed in the Matlab and Simulink environments. The hydraulic system consists of a high water head and a long penstock with upstream and downstream surge tanks, and is equipped with a Francis turbine. The nonlinear characteristics of hydraulic turbine and the inelastic water hammer effects were considered to calculate and simulate the hydraulic transients. With reference to the control solution, the proposed methodology relies on an adaptive control designed by means of the on-line identification of the system model under monitoring. Extensive simulations and comparison with respect to a classic hydraulic turbine speed PID regulator show the effectiveness of the proposed modelling and control tools.

## 1. Introduction

Hydroelectric plants convert hydraulic energy into useful energy (mainly electric and mechanical energy). Hydropower is, in fact, the most widely adopted form of renewable energy in the world today, accounting for approximately 16% of global energy production [1], *i.e.* 3673.1 TWh of energy are consumed from hydropower in various countries [2]. With increasing demand for electricity, and concern about reducing fossil fuel consumption, hydropower is likely to continue to play a key role in global energy production. Indeed, changing conditions in the power market have led to an increase in the demand of peak energy generation, short response time and fast frequency changes. Hydroelectric power plants thus need to be operated accounting for different load conditions. More in general, in the operation of hydropower systems the occurrence of variations in the flow is frequently experienced, being true either in routine operation, either in accidental or exceptional unforeseen events. The turbine operations such as start-up, load acceptance, load rejection and shutdown may result in hydraulic transients which can cause large pressure and sub-pressure oscillations in turbine hydraulic systems and must be evaluated to avoid mechanical failures. Consequently, there is a need for accurate simulation of transient flow in hydroelectric power plants and even though the basic technology in a plant has not changed much, powerful computers and software now allow the construction of virtual models and simulators of hydropower systems. Within this framework, Matlab and Simulink represent an interactive tool for modelling, simulating, and analysing dynamic systems which have been successfully applied also for nonlinear dynamics investigations in hydroelectric processes [3]. Furthermore, power plants are usually equipped with particular control systems to ensure stable operation. The satisfactory operation of a power system requires a frequency control that keeps



it within acceptable limits when the system undergoes significant load variation. The design of proper control systems for hydraulic turbines remains a challenging and important problem.

This paper considers the simulation and the control of a typical hydroelectric power plant, which has a high water head and a long penstock with upstream and downstream surge tanks, and is equipped with a Francis turbine [4]. The simulation model was developed in the Matlab and Simulink environments [5, 6]. The nonlinear characteristics of hydraulic turbine and the inelastic water hammer effect were considered to calculate and simulate hydraulic transients. The proposed control system is compared to a standard hydraulic turbine speed governor PID described and tuned in [3].

In the proposed control system, an electric servomotor is used as a governor [7, 8]. These solutions are preferable for the control of hydropower systems as they have a simple design, require less maintenance and are less expensive than conventional governors. Regarding the compensation strategy, several methodologies have been proposed in the literature [9]. For example, conventional control schemes are documented in [9]. Alternative control methods can be based *e.g.* on optimal control theory, which was exploited for adjusting the blade angles to achieve maximum operating efficiency at a given load [10]. Frequency control strategies were proposed *e.g.* in [11], whilst intelligent approaches relying *e.g.* on adaptive network based fuzzy inference system were addressed in [12].

With reference to the control strategy proposed in this work, the application of model identification mechanisms in connection with model-based adaptive control design has gained increasing attention [13]. The strategy suggested in this paper belongs to the field of adaptive control, which has undergone significant development in recent years. The aim of this approach is to solve the problem of controller design for instance where the characteristics of the process under investigation are not sufficiently known, or change over time. Since a mathematical model is a description of system behaviour, accurate modelling for a complex system is very difficult to achieve in practice. On-line or adaptive parametric model identification schemes represent an alternative for developing experimental models for complex systems. Because of these considerations, this paper suggests the implementation an adaptive controller based on an iterative identification scheme, used for the on-line estimation of the controlled process. While the process time-varying parameters have been estimated, the time-varying controller parameters are computed on-line, in order to maintain the required control performances. Thus, instead of exploiting complicated analytical nonlinear models, it is suggested to describe the plant under investigation by a parameter-varying linear model, whose variables are obtained by an on-line identification procedure. Note that the control strategy proposed here was exploited in a different framework, as described *e.g.* in [14, 15].

Extensive simulations under different working conditions are performed for the considered hydroelectric dynamic process. The achieved results indicate that the proposed methodology is effective to accurately describe the hydroelectric power plant nonlinear dynamics as well as to design a hydraulic turbine speed control system. The proposed simulation system may also be employed for preliminary designs or assessments of hydropower projects.

The paper has the following structure. Section 2 provides an overview of the hydroelectric dynamic process for modelling and control purposes. The proposed adaptive controller design and the tuning strategy are presented in Section 3.1, with reference to the identification of a discrete-time parameter-varying linear model. The on-line identification strategy exploited in this work for obtaining the input-output description of the considered hydraulic process is discussed in Section 3. The achieved results summarised in Section 4 show the performances of the control schemes, compared to a classic control strategy relying on a standard PID regulator. Section 5 concludes the paper by highlighting the main achievements of the work, open problems, and further investigations.

## 2. Hydraulic System Description

A general diagram of a hydroelectric power plant with two surge tanks is shown in Fig. 1 [3].

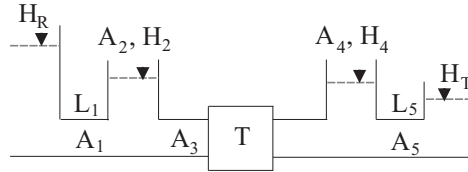


**Figure 1.** Layout of the simulated hydropower plant.

It consists of a reservoir with water level  $H_R$ , an upstream water tunnel with cross-section area  $A_1$  and length  $L_1$ , an upstream surge tank with cross-section area  $A_2$ , and water level  $H_2$ . This is followed by a downstream surge tank with cross-section area  $A_4$  and water level  $H_4$ , and a downstream tail water tunnel with cross-section area  $A_5$  and length  $L_5$ . Moreover, the penstock between hydraulic turbine and two surge tanks has a cross-section area  $A_3$  and length  $L_3$ . Finally, a tail water lake with water level  $H_T$  can be seen at the far right in Fig. 1. Reservoir water level  $H_R$  and tail water lake water level  $H_T$  are considered as constants.

Eqs. (1) and (2) express the non-dimensional flow rate and water pressure in terms of the corresponding relative deviations:

$$\frac{Q}{Q_r} = 1 + q \quad (1)$$

$$\frac{H}{H_r} = 1 + h \quad (2)$$

where  $q$  is the flow rate relative deviation, whilst  $h$  the water pressure relative deviation,

According to [3], with reference to a pressure water supply system, the Newton's second law for a fluid element inside a tube and the conservation mass law for a control volume, which accounts for water compressibility and tube elasticity, can be written. Under the assumption that the penstock is short or medium in length, water and pipeline can be considered incompressible and rigid, respectively. Therefore, only the inelastic water hammer effect can be taken into account. As shown in [3], the general expression can be simplified as:

$$\frac{h}{q} = -T_w s - H_f \quad (3)$$

Equation (3) represents the flow rate deviation and the water pressure deviation transfer functions for a simple penstock, where  $h$  is the water pressure relative deviation,  $q$  the flow rate relative deviation,  $H_f$  the hydraulic loss,  $s$  represents the Laplace operator, and  $T_w$  is the water inertia time given in Eq. (4):

$$T_w = \frac{L Q_r}{g A H_r} \quad (4)$$

The parameters that define the water inertia time  $T_w$  in Eq. (4) are the penstock length  $L$ , the rated flow rate  $Q_r$ , the gravity acceleration  $g$ , the cross-section area  $A$ , and the rated water pressure  $H_r$ . The typical hydroelectric power plant sketched in Fig. 1 can be divided into three sections: the upstream water tunnel, the penstock and the downstream tail water tunnel. The flow rate deviation and water pressure deviation transfer functions of the three sections are expressed in the following.

The upstream water tunnel connects the reservoir to the upstream surge tank. Since the inlet of upstream water tunnel is in reservoir and the water pressure deviation of the inlet is constant during hydraulic transients, the transfer function of the flow rate deviation and the water pressure deviation of the outlet of the upstream water tunnel can be expressed in the form:

$$\frac{h_1}{q_1} = -T_{w_1} s - H_{f_1} \quad (5)$$

The downstream tail water tunnel connects the downstream surge tank to the tail water lake. It is assumed that the outlet of the downstream tail water tunnel is in tailwater lake and the water pressure deviation of the outlet is constant. Therefore, the transfer function of flow rate deviation and the water pressure deviation of the inlet of downstream tail water tunnel has the form:

$$\frac{h_5}{q_5} = -T_{w_5} s - H_{f_5} \quad (6)$$

Usually, the water inertia in the draft tube is considered within the penstock. Thus, the transfer function of flow rate deviation (the subscript  $t$  refers to the turbine) and the water pressure deviation of the penstock can be written as:

$$h_t = h_2 - h_4 + h_3 \quad (7)$$

where:

$$\frac{h_3}{q_3} = -T_{w_3} s - H_{f_3} \quad (8)$$

The equations for the surge tanks are derived from the continuity of flow at the two junctions, where the hydraulic losses at orifices of surge tanks are neglected:

$$\begin{cases} \frac{A_2 H_r}{Q_r} \frac{dh_2}{dt} = q_2 = q_1 - q_3 \\ \frac{A_4 H_r}{Q_r} \frac{dh_4}{dt} = q_4 = q_3 - q_5 \end{cases} \quad (9)$$

The surge tank filling time can be expressed as:

$$T_s = \frac{A H_r}{Q_r} \quad (10)$$

The mathematical model and the performance curves of the Francis turbine considered in this paper were tuned in order to be compatible with the characteristics of the hydraulic system considered in [3]. The values of the main parameters of the hydraulic system and the Francis turbine at rated conditions are reported below:

- Reservoir water level  $H_r$ : 400 m;
- Water flow rate  $Q_r$ : 36.13 m<sup>3</sup>/s;
- Turbine power  $P_r$ : 127.6 MW;
- Turbine rotational speed  $n_r$ : 500 rpm.

Under these assumptions, the rated value of the efficiency  $\eta_r$  is equal to 90%, while the turbine-rated torque is 2437 kNm. The approach used to derive the non-dimensional performance curves adopted in this paper is different from the one followed in [3] and outlined in the following.

A second order polynomial curve, reported in Eq. (11), is used to relate the non-dimensional water flow rate  $Q/Q_r$  to the non-dimensional rotational speed  $n/n_r$ . The non-dimensional parameter  $G$ , which varies in the range 0 ÷ 100%, represents the wicket gate opening.

$$\frac{Q}{Q_r} = G \left[ a_1 \left( \frac{n}{n_r} \right)^2 + b_1 \left( \frac{n}{n_r} \right) + c_1 \right] = f_1(n, G) \quad (11)$$

The curve at  $G = 100\%$  (*i.e.* fully open wicket gate) is reported in Fig. 2, together with the curve at  $\eta = 0\%$ , so that the operating region allowed for the Francis turbine is defined. The water flow rate  $Q$  can be calculated by means of Eq. (11) for any operating point, as a function of the current rotational speed  $n$  and wicket gate opening  $G$ .

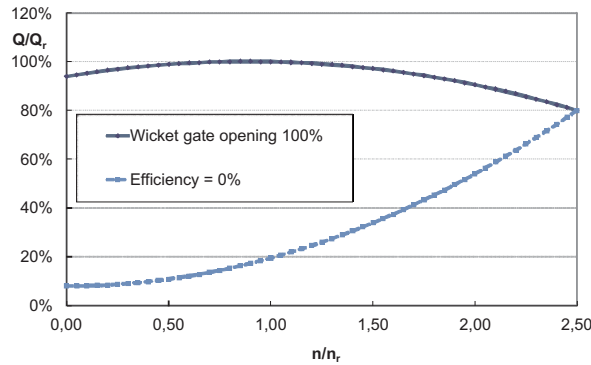


**Figure 2.** Non-dimensional water flow rate  $Q/Q_r$  vs. non-dimensional rotational speed  $n/n_r$ .

For the sake of simplicity, the turbine efficiency is assumed constant and equal to the rated value  $\eta_r$  (*i.e.* 90%). To account for the efficiency variation with the electric load, the turbine efficiency may be also expressed as a function of non-dimensional rotational speed (not considered in this paper). The non-dimensional turbine torque  $M$  is given by Eq. (12), as a function of the water flow rate  $Q$ , the water level  $H$  and the rotational speed  $n$ . According to the dependencies shown in Eq. (11), the turbine torque  $M$  is a function of the water flow rate  $Q$ , the rotational speed  $n$  and wicket gate opening  $G$ .

$$\frac{M}{M_r} = \frac{\frac{Q}{Q_r} \frac{H}{H_r}}{\frac{n}{n_r}} = f_2(Q, n, G) \quad (12)$$

Finally, as in [3], the relations of Eqs. (13) – (16) express all the non-dimensional parameters for the turbine in terms of the corresponding relative deviations. Note that, from the definition provided in Eq. (16), only negative values are allowed for  $y$ .

$$\frac{Q}{Q_r} = 1 + q_t \quad (13)$$

$$\frac{H}{H_r} = 1 + h_t \quad (14)$$

$$\frac{n}{n_r} = 1 + x \quad (15)$$

$$G = 1 + y \quad (16)$$

where  $q_t$  represents the turbine flow rate relative deviation,  $h_t$  the turbine water pressure relative deviation,  $x$  the turbine speed relative deviation, and  $y$  the wicket gate servomotor stroke relative deviation.

If the generator unit supplies an isolated load, then the dynamic process of the generator unit considering the load characteristic can be represented as:

$$\frac{x}{m_t - m_{g0}} = \frac{1}{T_a s + e_g} \quad (17)$$

where  $m_{g0}$  is the load torque,  $T_a$  the generator unit mechanical time, and  $e_g$  the load self-regulation factor.

In modern hydroelectric power plants, conventional PID control laws are applied to control the hydraulic turbine speed, where the control signal  $u$  is the sum of three elements of proportional, integral, and differential gain of hydraulic turbine speed deviation (error)  $x$ , which can be thus expressed as:

$$u = x \left( K_p + \frac{K_i}{s} + \frac{K_d s}{1 + T_n s} \right) \quad (18)$$

where  $K_p$  represents the proportional gain,  $K_i$  the integral gain,  $K_d$  the derivative gain,  $T_n$  the derivative filter time constant. Section 4 will analyse and compare the performance of this standard PID regulator designed in [3] with respect to the alternative control strategy proposed in this paper and described in Section 3.

Finally, with reference to the servomechanism of the process, by neglecting small time constants, the relationship between the control signal  $u$  and the wicket gate servomotor stroke  $y$  can be expressed by means of a first-order equation:

$$\frac{y}{u} = \frac{1}{T_y s + 1} \quad (19)$$

where  $T_y$  is the wicket gate servomotor response time.

### 3. Linear Parameter Varying Modelling for Control

This section describes the approach exploited for obtaining the mathematical description of the hydraulic system model, which is used for the design of the control strategy. In particular, the on-line identification scheme relying on the Least-Square Method (LSM) with adaptive directional forgetting discussed in [16] enhances the design procedure of the proposed adaptive controller, as shown in Section 3.1. This strategy represents an improvement with respect to classical LSM [17], and LMS with exponential forgetting [16].

The LSM with adaptive directional forgetting is thus used for the discrete-time on-line identification of processes that are described by the following transfer function  $G(z)$ :

$$G(z) = \frac{A(z^{-1})}{B(z^{-1})} = \frac{b_1 z^{-1} + \dots + b_m z^{-m}}{1 + a_1 z^{-1} + \dots + a_n z^{-n}} z^{-d} \quad (20)$$

where  $a_i$ ,  $b_i$ ,  $m$ ,  $n$ , and  $d$  represent the unknown parameters and the structure of the model, defining the polynomials  $A(z^{-1})$  and  $B(z^{-1})$ , whilst  $z$  is the discrete-time complex variable.

The estimated output of the process at the step  $k$ ,  $\hat{y}(k)$  is computed on the basis of the previous process input  $u$  and output  $y$  signals, according to (21):

$$\hat{y}(k) = -\hat{a}_1 y(k-1) - \dots - \hat{a}_n y(k-n) + \hat{b}_1 u(k-1-d) + \dots + \hat{b}_m u(k-m-d) \quad (21)$$

where  $\hat{a}_i$  and  $\hat{b}_i$  are the current estimations of process parameters at the step  $(k-1)$ . This equation can be written also in a vector form, as shown in (22) [17]:

$$\begin{aligned} \hat{y}(k) &= \Theta_{k-1}^T \Phi_k \\ \Theta_{k-1} &= [\hat{a}_1, \dots, \hat{a}_n, \hat{b}_1, \dots, \hat{b}_m]^T \\ \Phi_k &= [-y(k-1), \dots, -y(k-n), u(k-1-d), \dots, u(k-m-d)]^T \end{aligned} \quad (22)$$

The vector  $\Theta_{k-1}$  contains the model parameter estimates computed at the step  $(k-1)$ , whilst the vector  $\Phi_k$  contains the output and input values for the computation of the estimated output  $\hat{y}(k)$ . These vectors are used for describing the following identification method exploited for the on-line parameter estimation [16].

The LMS with adaptive directional forgetting scheme [16] is able to change the forgetting coefficient with respect to changes of the input and output signals. This method has been selected in this paper since it seems to improve the performances of LSM with exponential forgetting. Moreover, the main disadvantage of pure recursive LSM is the absence of any signal weighting. This feature is important when the actual process parameters change over time.

Thus, in the estimation scheme using *LSM with adaptive directional forgetting*, the process parameters are updated using the recursive expression:

$$\Theta_k = \Theta_{k-1} + \frac{C_{k-1} \Phi_k}{1 + \xi_k} \left( y(k) - \Theta_{k-1}^T \Phi_k \right) \quad (23)$$

where:

$$\xi_k = \Phi_k^T C_{k-1} \Phi_k \quad (24)$$

In each step  $k$ , the matrix  $C$  is updated according to (25):

$$C_k = \begin{cases} C_{k-1} - \frac{C_{k-1} \Phi_k \Phi_k^T C_{k-1}}{\epsilon_k^{-1} + \xi_k}, & \text{if } \xi_k > 0 \\ C_{k-1}, & \text{if } \xi_k = 0 \end{cases} \quad (25)$$

with:

$$\epsilon_k = \varphi_k - \frac{1 - \varphi_k}{\xi_{k-1}} \quad (26)$$

The forgetting coefficient  $\varphi_k$  is updated as follows:

$$\varphi_k = \frac{1}{1 + (1 + \rho) \left\{ \ln(1 + \xi_{k-1}) + \left[ \frac{(\nu_{k-1} + 1) \eta_{k-1}}{1 + \xi_{k-1} + \eta_{k-1}} - 1 \right] \frac{\xi_{k-1}}{1 + \xi_{k-1}} \right\}} \quad (27)$$

where:

$$\nu_k = \varphi_k (\nu_{k-1} + 1) \quad (28)$$

$$\eta_k = \frac{(y_k - \Theta_{k-1}^T \Phi_k)^T (y_k - \Theta_{k-1}^T \Phi_k)}{\lambda_k} \quad (29)$$

$$\lambda_k = \varphi_k \left[ \lambda_{k-1} + \frac{(y_k - \Theta_{k-1}^T \Phi_k)^T (y_k - \Theta_{k-1}^T \Phi_k)}{1 + \xi_{k-1}} \right] \quad (30)$$

are auxiliary variables.

The on-line identification method recalled here without using numeric filters was directly implemented in the Matlab<sup>®</sup> and Simulink<sup>®</sup> environments, as described in [13]. Note that the initial values of the parameters  $\Theta_0$ ,  $C_0$ ,  $\varphi_0$ ,  $\lambda_0$ ,  $\rho$ , and  $\nu_0$  have to be properly selected.

Finally, once the time-varying parameters of the discrete-time linear model approximating the behaviour of the whole continuous-time nonlinear dynamic process described in Section 2 have been computed at each time step  $k$ , the adaptive controller is designed as described in Section 3.1.



### 3.1. Adaptive Control Design

This section describes the adaptive control strategy used in connection with the on-line estimation scheme presented in Section 3. In more detail, with reference to the particular benchmark under diagnosis recalled in Section 2, a Ziegler–Nichols PI adaptive controller for processes of second order ( $n = 2$ ) is exploited [13].

With reference to (20), with  $n = m = 2$  and  $d = 0$ , the transfer function of the time-varying controlled system has the form:

$$G(z) = \frac{b_1 z^{-1} + b_2 z^{-2}}{1 + a_1 z^{-1} + a_2 z^{-2}} \quad (31)$$

whose parameters estimated using the on-line identification approach shown in Section 3 are:

$$\Theta_k = [\hat{a}_1, \hat{a}_2, \hat{b}_1, \hat{b}_2]^T \quad (32)$$

Therefore, the control law corresponding to a discrete-time Ziegler–Nichols PI adaptive controller has the form:

$$u(k) = K_p \left[ e(k) - e(k-1) + \frac{T_s}{T_I} \frac{e(k) - e(k-1)}{2} \right] + u(k-1) \quad (33)$$

where  $e(k)$  is the tracking error, *i.e.*  $e(k) = r(k) - y(k)$ , with  $r(k)$  the set-point or reference signal,  $T_s$  the sampling time. The controller variables  $K_p$  and  $T_I$  are computed from the time-varying model parameters  $\Theta_k$ . This type of control law can be transformed into its feedback representation:

$$u(k) = q_0 e(k) + q_1 e(k-1) + u(k-1) \quad (34)$$

The controller parameters  $q_0$  and  $q_1$  (or  $K_p$  and  $T_I$ ) are computed using following relations [18]:

$$\begin{aligned} q_0 &= K_p \left( 1 + \frac{T_s}{2T_I} \right), & q_1 &= -K_p \left( 1 - \frac{T_s}{2T_I} \right) \\ K_p &= 0.6 K_{P_u}, & T_I &= 0.5 T_u \end{aligned} \quad (35)$$

where the variables  $K_{P_u}$  and  $T_u$  are the critical gain and the critical period of oscillations, respectively. Also these variables are functions of the time-varying model parameters  $\Theta_k$

In particular, when considering a second order model described by its estimated parameters  $\hat{a}_2$ ,  $\hat{a}_1$ ,  $\hat{b}_2$ , and  $\hat{b}_1$ , the variables  $K_{P_u}$  and  $T_u$  required by the Ziegler–Nichols method can be computed at each time step  $k$  from the following relations [13]:

$$\begin{cases} K_{P_u} = \frac{\hat{a}_1 - \hat{a}_2 - 1}{\hat{b}_2 - \hat{b}_1} \\ T_u = \frac{2\pi T_s}{\arccos \gamma}, \quad \text{with } \gamma = \frac{\hat{a}_2 \hat{b}_1 - \hat{a}_1 \hat{b}_2}{2 \hat{b}_2} \end{cases} \quad (36)$$

In this way, the adaptive discrete-time linear controllers (33) or (34) are designed on the basis of the time-varying linear model (31) estimated via the on-line identification scheme from the data of the continuous-time nonlinear dynamic process described in Section 2.

## 4. Simulation Results

This section shows the achieved results regarding the design and the application of the adaptive controller to the sampled data acquired from the hydraulic model simulator. Note that the adaptive discrete-time controller is connected to the continuous-time controlled system via

analog to digital and digital to analog converters. The simulated system of the hydroelectric power plant described in Section 2 has been developed in the Matlab and Simulink environments.

As shown in Fig. 3, the complete model consists of three subsystems. First, the speed governors and servomechanism, in which turbine speed dead zone, valve saturation, and limitation are implemented. This subsystem provides the implementation of both the classic PID governor and the adaptive solution proposed in Section 3. As shown in Fig. 3 (a), through the parallel structure in Simulink, it is also possible to compare the performances of the two regulators. Note that the adaptive controller is connected to the controlled system via analog to digital and digital to analog converters, which are not shown in Fig. 3. Second, the hydrodynamics system (b) contains the tunnels, the penstock, and surge tanks. Third, the turbine generator and the network (c) represent the generator unit operating in isolation.

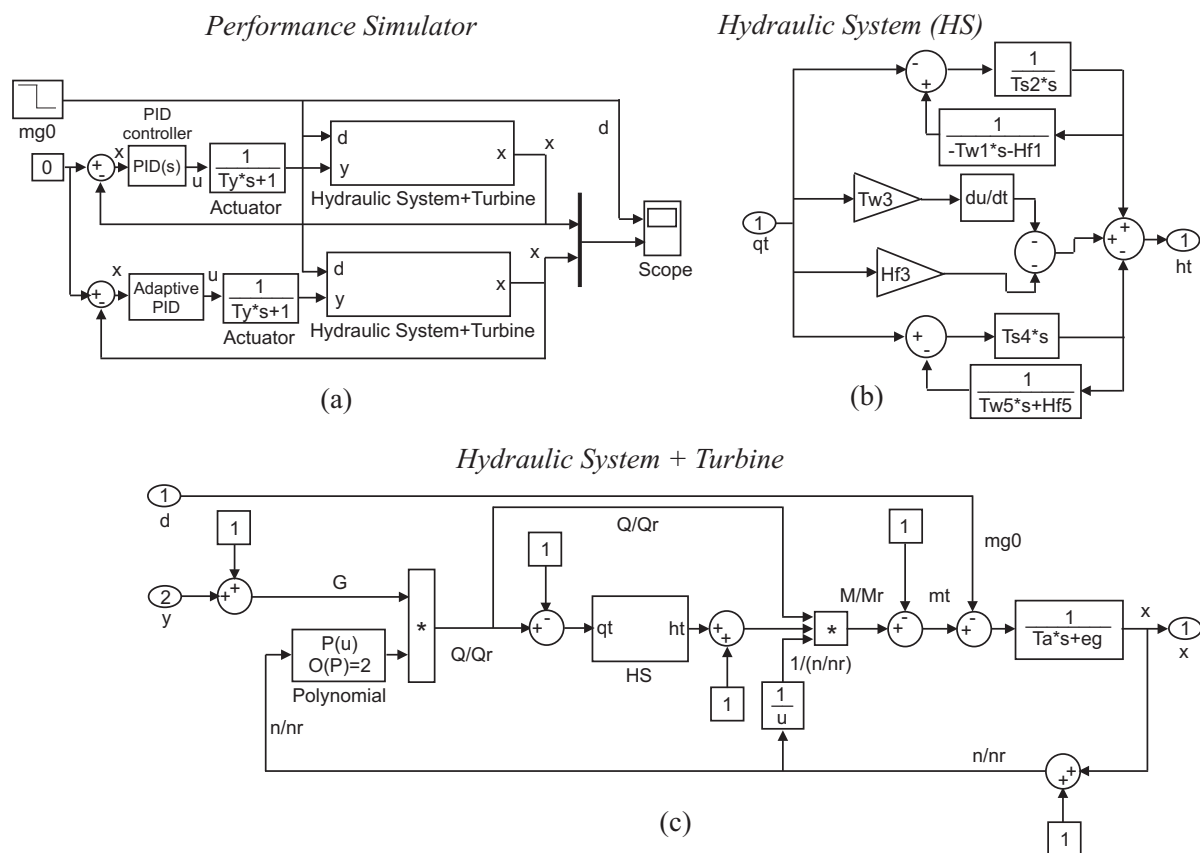


**Figure 3.** Simulink simulated systems: (a) speed controllers, servomechanism and hydrodynamic systems; (b) hydraulic system; (c) turbine, generator unit and network.

The simulation model with two surge tanks and a Francis turbine described in Fig. 3 should reflect the realistic behaviour of a hydroelectric power plant in the presence of large hydraulic transients after full load rejection  $m_{g0}$ . Usually, the most severe hydraulic transients will happen after full load rejection. Therefore, all of these simulations are performed on full load rejection operating conditions. The parameters of the model are summarised in Table 1.

The turbine speed governor plays a very important role in hydraulic transients caused by load changes. The classic PID controller proposed in [3] required an optimal tuning of its gains, and in this way only the dynamic performance of the generator unit can be improved. Moreover, in order to get the best dynamic performance, it is necessary to set different optimal PID gains on

different operating conditions for turbine speed governor.

**Table 1.** Simulated model parameters [3].

$H_{f_1} = 0.0481$	$H_{f_3} = 0.0131$	$H_{f_5} = 0.0047$	$T_c = 20$	$T_{s_2} = 476.05s$	$T_{s_4} = 5000s$
$T_{w_1} = 3.22s$	$T_{w_3} = 0.83s$	$T_{w_5} = 0.1s$	$a = -0.08$	$b = 0.14$	$c = 0.94$
$T_a = 5.9s$	$T_y = 0.5s$	$e_g = 0$	$K_d = 1.00$	$K_i = 0.20$	$K_p = 1.00$

On the other hand, a different method is proposed in Section 3 for the on-line modelling technique oriented to the design of the adaptive controller relying on the time-varying identified parametric model. Therefore, the output  $y$  of the continuous-time nonlinear hydraulic model described in Section 2 is approximated by a time-varying discrete-time prototype of the type of (31) with one input. Note that the model on-line estimation scheme presented in Section 3 is tested using different data sets. Therefore, the time-varying model parameters are estimated in order to minimise the so-called model-reality mismatch. In this way, the on-line estimated time-varying linear prototype should be able to provide the optimal fitting of all the working conditions of the hydraulic power plant, without the need of changing the controller parameters as required by the classic PID governor. Using this identified prototype, the model-based approach for determining the adaptive controller shown in Section 3.1 is exploited and applied to the hydraulic simulator described in Section 2. Thus, according to Section 3.1, the parameters of the adaptive controller have been computed. In particular, the identified time-varying prototype consist of a second order model; thus, the adaptive regulator parameters in (33) or (34) are computed analytically at each time step  $k$ .

It is worth highlighting the strategy applied for achieving the required adaptive characteristics. With reference to (33) or (34), the adaptive controller parameters are tuned via the Ziegler-Nichols rules, applied to the time-varying linear model, and by considering different working conditions. Therefore, the optimal controller performances with respect to set-point variations are thus enhanced. In this way, if both the model on-line parametric identification and the regulator tuning procedure are properly performed, the parameter adaptation mechanisms will lead to optimal adaptive properties. Moreover, by means of the proposed adaptation mechanisms, the suggested design scheme is able to maintain good control performances, even when conditions, different from those considered in [3], are simulated.

In the following, the suggested adaptive controller, together with the classic PID governor, have been implemented and compared in the Matlab and Simulink environments. The initial conditions for the on-line estimation algorithm (23)–(30) are listed in Table 2. Regarding the standard PID governor parameters in Eq. (18), they were selected as  $K_p = 1.0$ ,  $K_i = 0.2$ ,  $K_d = 1.0$ , and  $T_n = 0.01$  [3].

**Table 2.** Adaptive controller initialisation parameters.

$\Theta_0 = [0.1, 0.2, 0.3, 0.4]^T$	$C_0 = 10^9 I_4$	$\varphi_0 = 1$	$\lambda_0 = 0.001$	$\rho = 0.99$	$\nu_0 = 10^{-6}$
-------------------------------------	------------------	-----------------	---------------------	---------------	-------------------

The controller capabilities have been assessed in simulation by considering different load torque  $m_{g0}$  values. Fig. 4 shows the dynamics of the  $m_{g0}$  signal for the cases of +100% and -100%, which represent the turbine start-up and shutdown conditions, respectively. In particular, the start-up phase is assumed to last 300 s (due to the large size of the considered Francis turbine), while the shutdown maneuver takes just 30 s, to simulate an unplanned emergency shutdown. On the other hand, smaller  $m_{g0}$  variations analysed in the following have been modelled as step functions.

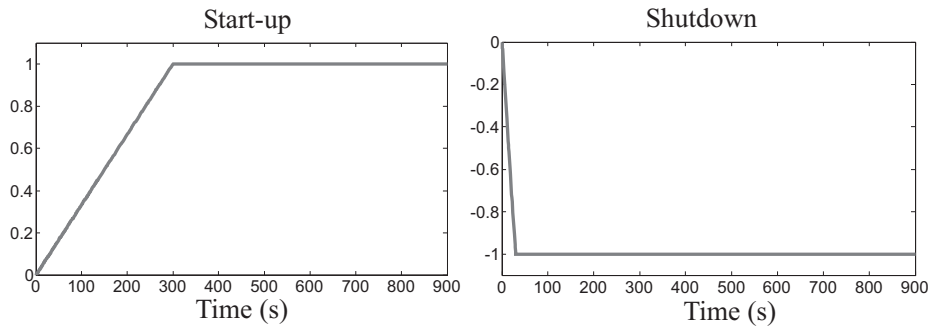


**Figure 4.**  $m_{g0}$  ramp functions for the turbine start-up and shutdown.

As an example, the results reported in Fig. 5 show that, even though both regulators can keep the relative deviation of the rotational speed null (*i.e.* the rotational speed constant) in steady-state conditions, the performances of the adaptive regulator of Eq. (34) are clearly better than those achievable by means of the standard PID governor of Eq. (18).

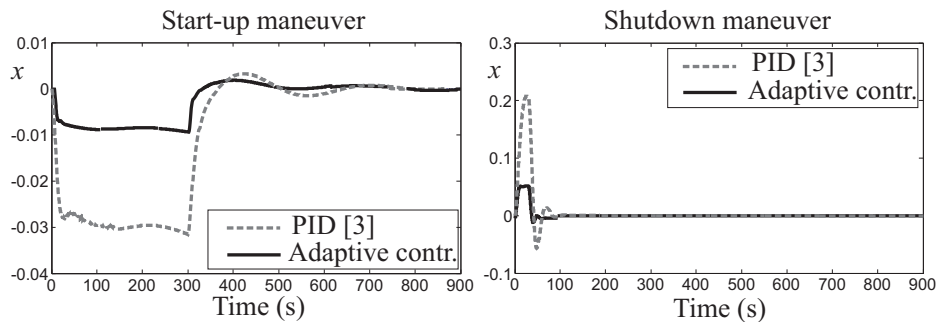


**Figure 5.** Turbine speed relative deviations  $x$  when the load torque  $m_{g0}$  changes in start-up and shutdown conditions.

In order to provide a comparison of the obtained performances, Table 3 summarises the achieved results in terms of per-cent Normalised Sum of Squared tracking Error ( $NSSE$ ) values defined as:

$$NSSE\% = 100 \sqrt{\frac{\sum_{k=1}^N x^2(k)}{N}} \quad (37)$$

that are computed with reference to the signal  $x$  for both the controllers for  $N$  samples. Moreover, the per-cent undershoot  $\sigma\%$ , overshoot  $S\%$  and the settling time  $T_s$  have been also estimated, for different values of the load torque  $m_{g0}$ .

According to these simulation results, good properties of the suggested adaptive controller are highlighted, and they are better than the standard PID governor. Some further comments

**Table 3.** Controllers'  $NSSE\%$ ,  $T_s$ ,  $\sigma\%$ , and  $S\%$ .

Controller Type	$m_{g0}$	$NSSE\%$	$T_s$	$\sigma\%$	$S\%$
Classic PID	+1%	0.04%	33.16s	0.38%	0.005%
	-1%	0.04%	31.39s	0.005%	0.39%
	+10%	0.39%	58.13s	3.75%	0.05%
	-10%	0.41%	27.57s	0.04%	3.95%
	+100%	1.86%	725.59s	3.15%	0.32%
	-100%	3.34%	76.05s	5.66%	20.73%
Adaptive Controller	+1%	0.037%	28.39s	0.33%	0.004%
	-1%	0.038%	27.13s	0.004%	0.36%
	+10%	0.38%	29.69s	2.37%	0.02%
	-10%	0.39%	18.64s	0.02%	1.78%
	+100%	0.62%	701.36s	0.96%	0.12%
	-100%	1.38%	54.08s	1.19%	5.76%

can be drawn in general regarding the capability of the adaptive controller. The  $NSSE$  values are usually comparable or slightly lower for reduced variations of the load torque, while they are considerably lower in case of significant transient maneuvers (*i.e.* start-up and shutdown). On the other hand, though always lower, the settling time  $T_s$  is not significantly decreased and remains comparable to that obtainable by means of the PID [3]. This is probably due to the inherent dynamics of the simulated hydraulic systems. Similarly, the per-cent  $\sigma\%$  and  $S\%$  are decreased in all cases by using the adaptive controller, and this effect is highlighted when considering the most severe transients (*i.e.* start-up and shutdown).

## 5. Conclusion

This paper addressed the design of an advanced control strategy for a hydroelectric power plant modelled in the Matlab and Simulink environments. The hydraulic system consisted of a high water head and a penstock with upstream and downstream surge tanks and a Francis turbine. The nonlinear characteristics of hydraulic model were considered to simulate the hydraulic transients and to evaluate the behaviour of the proposed hydraulic turbine regulating system. The suggested control methodology was based on an adaptive control designed by means of the on-line identification of the system model under monitoring. Extensive simulations showed the main features of the proposed modelling and control tools, as well as highlighted its benefit mainly in correspondence of the most severe transients. The considered simulation tools could be also useful for preliminary designs or assessments of the most important features of hydropower installations and their control strategies.

## References

- [1] I. Working Group III Mitigation of Climate Change, "Special Report on Renewable Energy Sources and Climate Change Mitigation," tech. rep., Intergovernmental Panel on Climate Change, 2011.
- [2] R. R. Singh, T. R. Chelliah, and P. Agarwal, "Power electronics in hydro electric energy systems – A review," *Renewable and Sustainable Energy Reviews*, vol. 32, pp. 944–959, April 2014.
- [3] H. Fang, L. Chen, N. Dlakavu, and Z. Shen, "Basic modeling and simulation tool for analysis of hydraulic transients in hydroelectric power plants," *IEEE Trans. Energy Convers.*, vol. 23, pp. 424–434, Sept. 2008.
- [4] M. Popescu, D. Arsenie, and P. Vlase, *Applied Hydraulic Transients: For Hydropower Plants and Pumping Stations*. Lisse, The Netherlands: CRC Press, Jan. 2003.

- [5] C. D. Vournas and G. Papaionnou, “Modeling and stability of a hydro plant with two surge tanks,” *IEEE Trans. Energy Convers.*, vol. 10, pp. 368–375, Jun.
- [6] D. N. Konidaris and J. A. Tegopoulos, “Investigation of oscillatory problems of hydraulic generating units equipped with francis turbines,” *IEEE Trans. Energy Convers.*, vol. 12, pp. 419–425, Dec. 1997.
- [7] *Power System Control & Stability*, vol. 111 of *IEEE Series Power Eng.* River Street, Hoboken, NJ: John Wiley and Sons, Inc., 2003.
- [8] M. Hanmandlu and H. Goyal, “Proposing a new advanced control technique for micro hydro power plants,” *Electrical Power and Energy Systems*, vol. 30, 2008. DOI: doi:10.1016/j.ijepes.2007.07.010.
- [9] J. A. Laghari, H. Mokhlis, A. H. A. Bakar, and H. Mohammad, “A comprehensive overview of new designs in the hydraulic, electrical equipments and controllers of mini hydro power plants making it cost effective technology,” *Renewable and Sustainable Energy Reviews*, vol. 20, pp. 279–293, 2013.
- [10] P. Schniter and L. Wozniak, “Efficiency based optimal control of kaplan hydro generators,” *IEEE Trans. Energy Convers.*, vol. 10, pp. 348–353, June 1995.
- [11] O. P. Malik, G. S. Hope, G. C. Hancock, L. Zhaohui, Y. Luqing, and W. E. I. Shouping, “Frequency measurement for use with a microprocessor based water turbine governor,” *IEEE Trans. Energy Convers.*, vol. 6, pp. 361–366, Sept. 1991.
- [12] M. Djukanovic, M. Novicevic, D. J. Dobrijevic, B. Babic, J. Dejan, and Y. H. P. Sobajic, “Neural-net based coordinated stabilizing control for the exciter and governor loops of low head hydropower plants,” *IEEE Trans. Energy Convers.*, vol. 10, pp. 760–767, Dec. 1995.
- [13] V. Bobál, J. Böhm, J. Fessler, and J. Macháček, *Digital Self-Tuning Controllers: Algorithms, Implementation and Applications*. Advanced Textbooks in Control and Signal Processing, Springer, 1st ed., 2005.
- [14] S. Simani, “Application of a Data-Driven Fuzzy Control Design to a Wind Turbine Benchmark Model,” *Advances in Fuzzy Systems*, vol. 2012, pp. 1–12, November 2nd 2012. Invited paper for the special issue: Fuzzy Logic Applications in Control Theory and Systems Biology (FLACE). ISSN: 1687-7101, e-ISSN: 1687-711X. DOI: 10.1155/2012/504368.
- [15] S. Simani and P. Castaldi, “Data-Driven and Adaptive Control Applications to a Wind Turbine Benchmark Model,” *Control Engineering Practice*, vol. 21, pp. 1678–1693, December 2013. Special Issue Invited Paper. ISSN: 0967-0661. PII: S0967-0661(13)00155-X. DOI: <http://dx.doi.org/10.1016/j.conengprac.2013.08.009>.
- [16] R. Kulhavý, “Restricted exponential forgetting in real-time identification,” *Automatica*, vol. 23, no. 9, pp. 589–600, 1987.
- [17] L. Ljung, *System Identification: Theory for the User*. Englewood Cliffs, N.J.: Prentice Hall, second ed., 1999.
- [18] K. J. Astrom and T. Hagglund, *PID Controllers*. Instrument Society of America, 1995.